Single-, double-, and triple-photoionization cross sections of carbon monoxide (CO) and ionic fragmentation of CO^+, CO^{2+}, and CO^{3+}

Toshio Masuoka
Department of Applied Physics, Faculty of Engineering, Osaka City University, Sugimoto 3, Sumiyoshi-ku, Osaka 558, Japan

Eiken Nakamura
Ultraviolet Synchrotron Orbital Radiation Facility, Institute for Molecular Science, Myodaiji, Okazaki 444, Japan
(Received 15 July 1993)

Single-, double-, and triple-photoionization processes of carbon monoxide (CO) have been studied in the photon-energy region of 37–100 eV by use of time-of-flight mass spectrometry and a photoion-photoion-coincidence method together with synchrotron radiation. The single-, double-, and triple-photoionization cross sections of CO are determined. Ion branching ratios and the partial cross sections for the individual ions respectively produced from the precursors CO^+ and CO^{2+} are determined separately at excitation energies where the molecular and dissociative single- and double-photoionization processes compete. The threshold for the molecular double photoionization was found to be 41.3 ± 0.2 eV. Furthermore, in single photoionization, the production of CO^+ is dominant whereas with double photoionization dissociation becomes dominant.

PACS number(s): 33.80.Eh, 33.80.Gj

I. INTRODUCTION

In recent years, considerable attention has been directed to diatomic molecular dications such as CO^{2+} and NO^{2+} both experimentally and theoretically [1,2]. Lablanquie *et al.* [2] studied the spectroscopy and the dynamics of CO^{2+} and CO^{3+} using various complementary experiments, such as mass spectrometric photoionization with synchrotron radiation, photoion-photoion-coincidence technique (PIPICO), and H^+ double-charge-transfer spectroscopy. They reported partial cross sections for the molecular (CO^{2+}) and dissociative double ($C^+ + O^+$) and triple ($C^{2+} + O^+$) photoionization, normalizing their data to the absolute cross section previously reported [3], which unfortunately was subject to discrimination effects against energetic photoelectrons. Becker *et al.* [4] reported the results of photoelectron spectroscopy, and they concluded that three processes are in competition in the dissociative double photoionization of CO: (a) direct double ionization, (b) indirect double ionization followed by dissociation, and (c) direct dissociation of the molecular ion with subsequent relaxation in the excited atom. They further reported the ratio of double to single ionization in the region 50–120 eV.

Although molecular double ionization is usually followed by the production of an ion pair ($A^+ + B^+$, dissociative double ionization) when excitation energy exceeds the double-photoionization threshold by a few electron volts, both molecular and dissociative double ionization are, in general, not accurately estimated in the determination of double-photoionization cross section. To address this problem, the present study focuses on the determination of the partial cross sections for the single, double, and triple photoionization of carbon monoxide at excitation energies where molecular and dissociative single, double, and triple photoionization takes place concomitantly. This is because the probability of two-electron ejection is important in the understanding of electron correlations, and an accurate determination of the partial cross sections should be extended to molecules in which various processes are in competition to further clarify the correlations.

In the present study, the time-of-flight (TOF) mass spectrometry and PIPICO methods were used together with synchrotron radiation. It is necessary to use two such complementary experimental methods to determine the partial cross sections because TOF mass spectra provide only the ion branching ratios for the final ionic products originating from the precursors AB^+, AB^{2+}, and AB^{3+} in a microsecond time scale and PIPICO spectra provide only the intensity of dissociation channels, $A^+ + B^+$ of AB^{2+} and $A^{2+} + B^+$ of AB^{3+}. The ratio of the molecular to the dissociative processes is usually not known. Consequently, to determine the partial cross sections for single, double, and triple photoionization when the molecular and dissociative processes are in competition, a method to bridge the TOF and PIPICO spectra was recently developed and applied to nitric oxide [5] and carbonyl sulfide [6]. This method is herein applied to the molecular and dissociative single, double, and triple photoionization of carbon monoxide. Ion branching ratios and the partial cross sections for the individual ions produced from the precursors CO^+ and CO^{2+} are also separately determined.

Previous investigations on CO^{2+} include photon and electron impact ionization mass spectrometry [2,3,7–12], Auger spectroscopy [13–15], translational energy spectroscopy (TES) [16–20], double-charge-transfer spectroscopy (DCTS) [2,20–23], photoion-photon-of-fluorescence coincidence measurements (PIFCO) [24], coincidence measurements of a cation pair (PIPICO for photoionization) [2,25], kinetic-energy-release measurements

[24,26,27], photoelectron spectroscopy [4], and theoretical calculations [2,15,20,28–32]. A brief review of theoretical and experimental work on CO^{2+} prior to 1993 can be found in Ref. [23]. Although the appearance potential of CO^{2+} in the literature ranges from 39.5 to 41.8 eV, the closest estimation to date seems to be 41.4±0.4 eV [23].

II. EXPERIMENTAL PROCEDURE

The photoionization mass spectra and PIPICO spectra were measured with the use of a TOF mass spectrometer, the details of which have been described elsewhere [33,34]. A relatively high dc electric field (2250 V/cm) was applied across the ionization region and the potential of the drift tube and the ion detector was kept at −4500 V. The TOF mass spectra and the PIPICO spectra were measured at an angle of ~50° with respect to the polarization vector where the second-order Legendre polynomial is close to zero. Under these conditions, the effects of anisotropic angular distributions of fragment ions are minimized [35]. The absolute collection efficiencies of energetic fragment ions in the TOF mass spectrometer calculated with a computer program indicate that no conditions exist under which all ion pairs are collected, even if the total kinetic energy of fragment ions is smaller than 1 eV (collection efficiency of 96%) and the efficiency for the fragment ions with a total kinetic energy of 20 eV is 80%.

The TOF mass spectrometer was operated in two modes for the measurement of TOF mass spectra. In mode A, the photoelectron signal detected by the channel electron multiplier was fed into the start input of a time-to-amplitude converter (TAC). The storage ring was operated in a multibunch mode. In this mode of operation of the TOF mass spectrometer, the relative ion yields in single and double photoionization are affected by the different kinetic energies of each photoelectron and the different number of photoelectrons in the two processes. Triple photoionization is ignored here for simplicity because it is a very weak process. At 60 eV, for example, the kinetic energy of photoelectrons ejected forming the ground state of CO^+ is of the order of 46 eV, whereas that forming the ground state of CO^{2+} is about 20 eV. These more energetic photoelectrons produced by single photoionization are more easily discriminated in the TOF mass spectrometer than those produced by double photoionization. This discrimination effect results in an underestimation of the number of ions produced by single photoionization. In contrast, the different number of ejected electrons in single and double photoionization causes an overestimation of the number of ions produced in double photoionization because the probability of forming one output pulse is higher for two electrons hitting simultaneously than for one electron [6]. A typical TOF mass spectrum measured at $h\nu=60$ eV is shown in Fig. 1.

In mode B, the rf frequency (90.115 MHz) of the storage ring was used as the start signal of the TAC by reducing it to $\frac{1}{32}$ through a frequency demultiplier. The storage ring was operated in a single-bunch mode, which was essential to obtain meaningful TOF mass spectra. A typical TOF mass spectrum measured at $h\nu=80$ eV is shown in Fig. 2 which is complicated because two or three bunches pass in front of the beam line in the time range shown in the figure and corresponding sets of the mass spectrum are recorded. In mode B, it is believed that the observed mass spectra are free from the discrimination effects mentioned above because the ratio of the partial cross sections $\sigma(Ar^{2+})/\sigma(Ar^+)$ measured in the region from the double-photoionization threshold to 100 eV was in good agreement with previous reports [36].

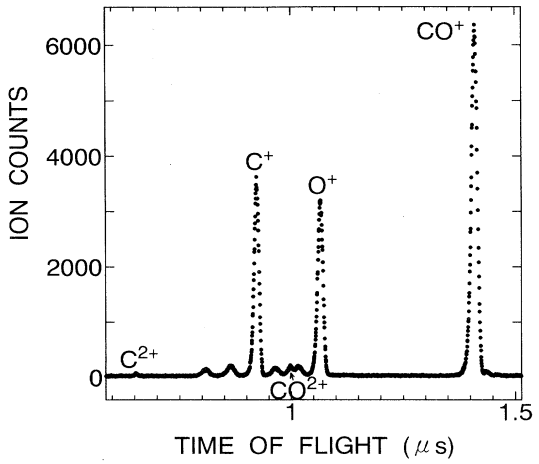

FIG. 1. Time-of-flight mass spectrum measured at a photon energy of 60 eV by using the photoelectron signal as the start input of a TAC (mode A). The two broad humps between the C^{2+} and C^+ peaks and those between C^+ and O^+ occurring at higher photon energies are unidentified.

Monochromatic radiation was provided by a constant-deviation grazing incidence monochromator installed at the UVSOR (UltraViolet Synchrotron Orbital Radiation) facility of IMS (the Institute for Molecular Science) in Okazaki and an Al optical filter (for 37–70 eV; no filter

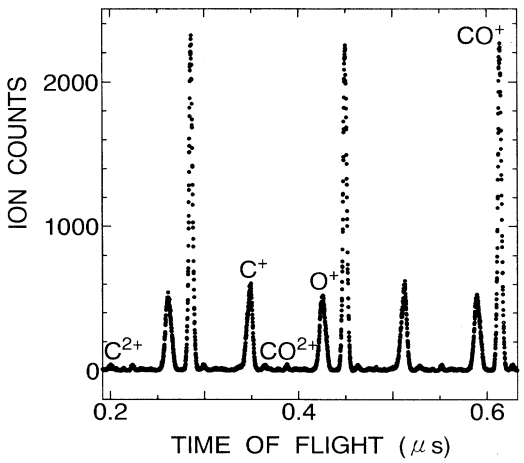

FIG. 2. Time-of-flight mass spectrum measured at a photon energy of 80 eV by using the rf frequency as the start input of a TAC (mode B). The spectrum is complicated because of the presence of two or three mass peaks, each corresponding to one particular type of ion.

above 70 eV). The bandpass of the monochromator was about 0.4 Å with 100-μm-wide entrance and exit slits.

III. DATA ANALYSIS

The method used for data analysis was described previously for nitric oxide [5] and carbonyl sulfide [6]. Because the reliable ion branching ratios for CO were obtained in mode B (Sec. II), the method should be slightly modified. The ion branching ratios measured in the multibunch mode were carefully normalized to those measured in the single-bunch mode and then analyzed. The overall scheme of photoionization and subsequent dissociation is represented by

$$\mathrm{CO}+h\nu\rightarrow\mathrm{CO}^{+}(N_s)\rightarrow\mathrm{C}_s^{+},\mathrm{O}_s^{+}\quad(\xi_s)\,, \tag{1a}$$

$$\rightarrow\mathrm{CO}^{+}\quad(1-\xi_s)\,, \tag{1b}$$

$$\rightarrow\mathrm{CO}^{2+}(N_d)\rightarrow\mathrm{C}_d^{+}+\mathrm{O}_d^{+}\quad(\xi_d)\,, \tag{1c}$$

$$\rightarrow\mathrm{C}_d^{2+},\mathrm{O}_d^{2+}\quad(\xi_d)\,, \tag{1d}$$

$$\rightarrow\mathrm{CO}^{2+}\quad(1-\xi_d-\zeta_d)\,, \tag{1e}$$

$$\rightarrow\mathrm{CO}^{3+}(N_t)\rightarrow\mathrm{C}_t^{2+}+\mathrm{O}_t^{+}\quad(\xi_t=1)\,, \tag{1f}$$

where N_s, N_d, and N_t represent the rates of single, double, and triple photoionization, respectively; and ξ_s, $\xi_d+\zeta_d$, and ξ_t are the ratios of dissociative single, double, and triple photoionization, respectively. Although the dissociation of CO^{3+} into $\mathrm{C}^{+}+\mathrm{O}^{2+}$ may be possible [37], this process was ignored because this peak appeared very close to the intense peak of $\mathrm{C}^{+}+\mathrm{O}^{+}$ in the PIPICO spectra and it was, therefore, difficult to measure.

A. Determination of single-, double-, and triple-photoionization cross sections

The single-, double-, and triple-photoionization cross sections σ^{+}, σ^{2+}, and σ^{3+} were obtained as a function of excitation energy. The ratio of double to single photoionization is given by

$$\frac{N_d}{N_s}=\frac{1}{f_i I(\xi_d+N_t/N_d)/C_{II}-(1+\xi_d+2N_t/N_d)}\,, \tag{2}$$

where f_i is the ion-detection efficiency (ion collection efficiency in the TOF plus detection efficiency), I is the ion count rate, and C_{II} is the ion-ion-coincidence rate obtained by integrating the PIPICO peaks over all ion-pair processes. The apparent ion branching ratio $R_A(\mathrm{CO}^{2+}+\mathrm{C}^{2+}+\mathrm{O}^{2+})$ for the doubly charged CO^{2+}, C^{2+}, and O^{2+} ions obtained directly from the mass spectrum is given by

$$R_A(\mathrm{CO}^{2+}+\mathrm{C}^{2+}+\mathrm{O}^{2+})=\frac{(1-\xi_d)N_d}{N_s+(1+\xi_d)N_d+2N_t}\,. \tag{3}$$

For all practical purposes, N_t in Eqs. (2) and (3) can be ignored because the maximum value of the ratio $N_t/\xi N_d$ is only 0.022 at 100 eV. The ratio of triple to double photoionization is obtained from the PIPICO branching ratio R_P under the assumption that the precursor CO^{3+} completely dissociates to $\mathrm{C}^{2+}+\mathrm{O}^{+}$, that is,

$$\frac{N_t}{N_d}=\frac{R_P(\mathrm{triple})}{1-R_P(\mathrm{triple})}\xi_d\equiv\alpha\xi_d\,, \tag{4}$$

where $R_P(\mathrm{triple})$ is the PIPICO branching ratio for triple photoionization. From these equations, ξ_d, for example, is given by

$$\xi_d=\frac{x-R_A-xR_A}{(R_A+\alpha R_A+1)x}\,, \tag{5}$$

where $x=N_d/N_s$.

These rates (N_s, N_d, and N_t) were converted to the cross sections of single, double, and triple photoionization by using the total photoionization cross sections reported by Samson and co-workers [38,39] as a function of excitation energy. The data reported by Samson and coworkers were considered reliable because it is in excellent agreement with data recently reported by Chan, Cooper, and Brion [40].

B. Determination of the ion branching ratios and the partial cross sections for the fragmentation of CO^{+}, CO^{2+}, and CO^{3+}

The apparent ion branching ratio $R_A(\mathrm{O}^{+})$ for the O^{+} fragment ion obtained directly from the mass spectrum at higher photon energies is the sum of the values for single (O_s^{+}), double (O_d^{+}), and triple (O_t^{+}) photoionization. That is,

$$R_A(\mathrm{O}^{+})=R_A(\mathrm{O}_s^{+})+R_A(\mathrm{O}_d^{+})+R_A(\mathrm{O}_t^{+})\,. \tag{6}$$

The three terms on the right-hand side in Eq. (6) are apparent ion branching ratios that are related to the inherent ion branching ratios $R(\mathrm{O}_s^{+})$, $R(\mathrm{O}_d^{+})$, and $R(\mathrm{O}_t^{+})$ for the O_s^{+}, O_d^{+}, and O_t^{+} ions, respectively (from the precursors CO^{+}, CO^{2+}, and CO^{3+}) by the following equations:

$$R_A(\mathrm{O}_s^{+})=\frac{N_s}{N_s+(1+\xi_d)N_d+2N_t}R(\mathrm{O}_s^{+})\,, \tag{7}$$

$$R_A(\mathrm{O}_d^{+})=\frac{N_d}{N_s+(1+\xi_d)N_d+2N_t}R(\mathrm{O}_d^{+})\,, \tag{8}$$

$$R_A(\mathrm{O}_t^{+})=\frac{N_t}{N_s+(1+\xi_d)N_d+2N_t}R(\mathrm{O}_t^{+})\,. \tag{9}$$

From the overall scheme of photoionization and dissociation [Eq. (1)], $R(\mathrm{O}_d^{+})=\xi_d$ and $R(\mathrm{O}_t^{+})=1$. Thus $R_A(\mathrm{O}_d^{+})$ and $R_A(\mathrm{O}_t^{+})$ can be determined directly from Eqs. (8) and (9), respectively. $R_A(\mathrm{O}_s^{+})$ is determined from Eq. (6), and by substituting the result into Eq. (7) we can finally determine $R(\mathrm{O}_s^{+})$. These equations are essentially the same as those in Ref. [6], if f_s, f_d, and f_t (the electron-detection efficiencies for one, two, and three electrons ejected in single, double, and triple photoionization, respectively) are omitted in Ref. [6].

IV. RESULTS AND DISCUSSION

A. Ion branching ratios

The apparent ion branching ratios directly obtained from the mass spectra measured in modes A and B are

shown in Fig. 3, and are compared with those reported by Wight, Van der Wiel, and Brion [7], and Masuoka and Samson [3]. Figures 3(a) and 3(b) illustrate that the present results obtained in mode A are in good agreement (within about 10%) with the data reported by Masuoka and Samson [3]. This is because both measurements used the photoelectron signal as the start input of a TAC and therefore, both measurements were influenced by the discrimination effects against photoelectrons. The slight discrepancy between the two sets of data may be due to different sensitivities of the ion detectors used and different settings of the mass spectrometers with respect to the polarization vector (Masuoka and Samson measured the mass spectra in a horizontal plane [3]).

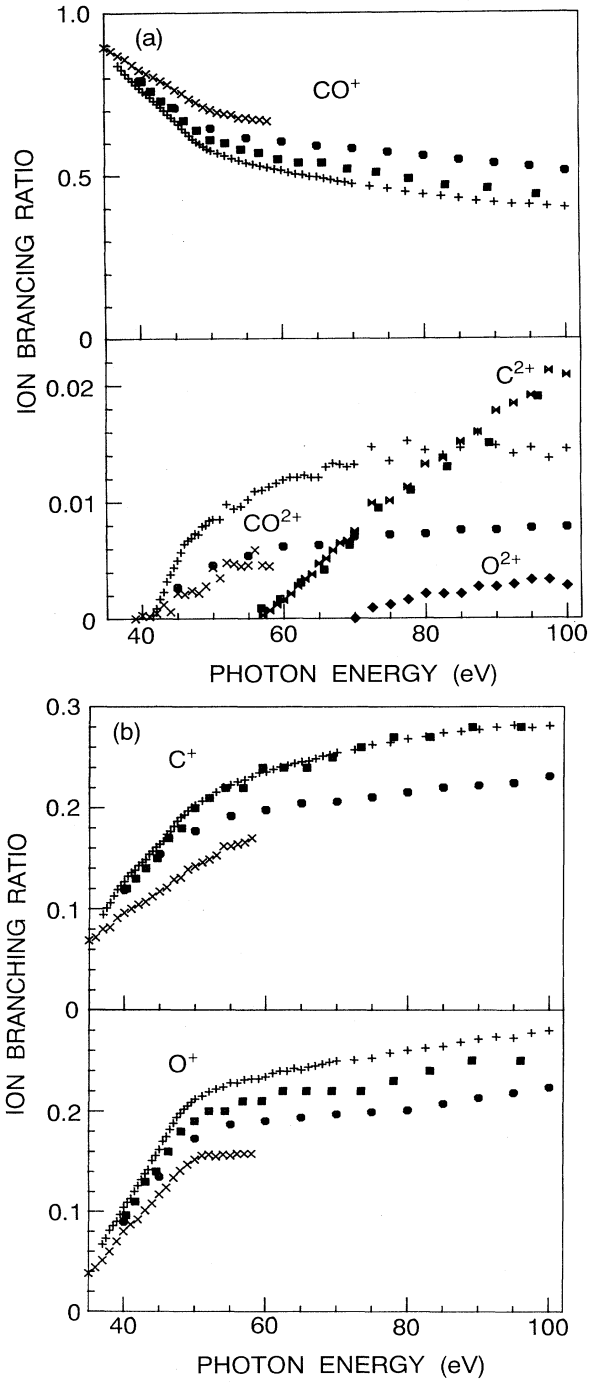

FIG. 3. Ion branching ratios directly obtained from the mass spectra as a function of photon energy. +, ⋈, and ♦ (mode A) and ● (mode B), present data; ■, from Ref. [3]; ×, from Ref. [7].

The present results obtained in mode A are 12% lower for CO^+, 22% higher for C^+, and 27% higher for O^+ at 100 eV than those measured in mode B. However, the change in the apparent ion branching ratios measured in the two modes for CO^{2+} is drastic: the results in mode A are about 90% higher than those in mode B throughout the energy region studied. This clearly demonstrates the inadequacy of using the photoelectron signal as the start input of a TAC. The apparent ion branching ratios for the molecular CO^{2+} ion measured in mode B are in good agreement with the data reported by Wight, Van der Wiel, and Brion [7] except for poor counting statistics in the latter. The data reported by Wight, Van der Wiel, and Brion are 10% higher for CO^+, 16% lower for C^+, and 17% lower for O^+ at 55 eV than the present results measured in mode B. These discrepancies are not clear at present. It should be mentioned, however, that the results obtained for nitric oxide in mode B are in good agreement (within 5%) with those obtained by the dipole (e, e+ion) method (Iida *et al*, [41]) except for O^+, for which discrepancies of 16–26% were observed in the 60–80-eV region.

B. Single-, double-, and triple-photoionization cross sections

The ratios of double to single and of triple to single photoionization determined by the method described in Sec. III A are shown in Fig. 4 and listed in Table I. The absolute cross sections for the single, double, and triple photoionization shown in Fig. 5 (Table I) were obtained from the total cross section σ_t [38,39] assuming that $\sigma_t = \sigma^+ + \sigma^{2+} + \sigma^{3+}$. It is emphasized that the double-photoionization cross section shown in Figs. 4 and 5 includes both the molecular and dissociative processes of the precursor CO^{2+}.

As for the ratio of σ^{2+}/σ^+, Lablanquie *et al.* [2] re-

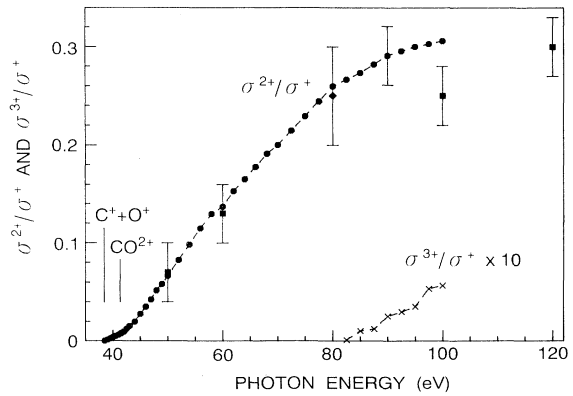

FIG. 4. Ratios of double- (σ^{2+}) to single- (σ^+) and triple- (σ^{3+}) to single-photoionization cross section of CO. ● and ×, present data; ■, from Ref. [4]; ♦, from Ref. [2].

ported the value of about 0.25 at 80 eV from their photoionization data measured with synchrotron radiation. Becker *et al.* [4] have estimated the ratio in the region of 50–120 eV from their photoelectron spectra. Those are shown in Fig. 4 for comparison. If 10% uncertainty is assumed in the present data, as shown at 90 eV in the figure, excellent agreement can be found among the three sets of data.

It has been observed by Lablanquie *et al.* [2] and Mathur and Eland [12] that the dissociative double photoionization ($C^+ + O^+$) takes place below the molecular double photoionization with the threshold at 38.4±0.5 eV [2]. A similar result was also observed in the present experiment with a threshold very close to the reported value. Because the threshold (38.4±0.5 eV) was deduced from their densely measured data, the same value was adopted as the threshold of double photoionization in the present study. Lablanquie *et al.* [2] proposed an indirect process that highly excited $(CO^*)^+$ states (Rydberg states converging to the CO^{2+} states) autoionize to the lowest dissociative $^3\Sigma^-$ state of CO^{2+} at large internuclear distances. They further eliminated the contribution of double Rydberg states (CO^{**}) on the basis of the kinetic-energy-release distributions (KERD's) at higher photon energies. However, if one considers a high density of the CO^{2+} electronic states and competition of various double-ionization processes [4], it would be possible to produce the $C^+ + O^+$ ion pair with low kinetic energies from resonance processes at higher photon energies. Therefore it seems likely that double Rydberg states

TABLE I. Partial cross sections for the single, double, and triple photoionization of CO and their ratios.

Photon energy (eV)	σ^+ (Mb)	σ^{2+} (Mb)	σ^{3+} (kb)	σ^{2+}/σ^+	σ^{3+}/σ^+
37.0	13.10				
37.5	12.96				
38.0	12.81				
38.5	12.66	0.001		0.0001	
39.0	12.50	0.015		0.0012	
39.5	12.32	0.030		0.0024	
40.0	12.11	0.045		0.0037	
40.5	11.91	0.059		0.0049	
41.0	11.70	0.072		0.0061	
41.5	11.55	0.090		0.0078	
42.0	11.37	0.11		0.0095	
42.5	11.17	0.14		0.012	
43.0	10.97	0.17		0.015	
44.0	10.74	0.21		0.020	
45.0	10.46	0.29		0.028	
46.0	10.18	0.36		0.035	
47.0	9.86	0.42		0.042	
48.0	9.52	0.49		0.052	
49.0	9.25	0.54		0.058	
50.0	8.96	0.60		0.066	
52.0	8.21	0.68		0.082	
54.0	7.53	0.74		0.098	
56.0	6.90	0.79		0.115	
58.0	6.35	0.82		0.129	
60.0	5.92	0.81		0.137	
62.0	5.46	0.84		0.153	
64.0	5.04	0.83		0.165	
66.0	4.65	0.83		0.178	
68.0	4.32	0.83		0.191	
70.0	4.07	0.81		0.200	
72.5	3.75	0.80		0.215	
75.0	3.42	0.78		0.229	
77.5	3.14	0.77		0.244	
80.0	2.93	0.76		0.260	
82.5	2.75	0.73	0.3	0.266	0.0001
85.0	2.57	0.70	2.7	0.273	0.0010
87.5	2.41	0.68	3.0	0.282	0.0013
90.0	2.23	0.65	5.7	0.291	0.0026
92.5	2.15	0.64	6.5	0.296	0.0030
95.0	1.97	0.59	7.0	0.300	0.0035
97.5	1.86	0.56	9.9	0.303	0.0054
100.0	1.77	0.54	10.0	0.306	0.0057

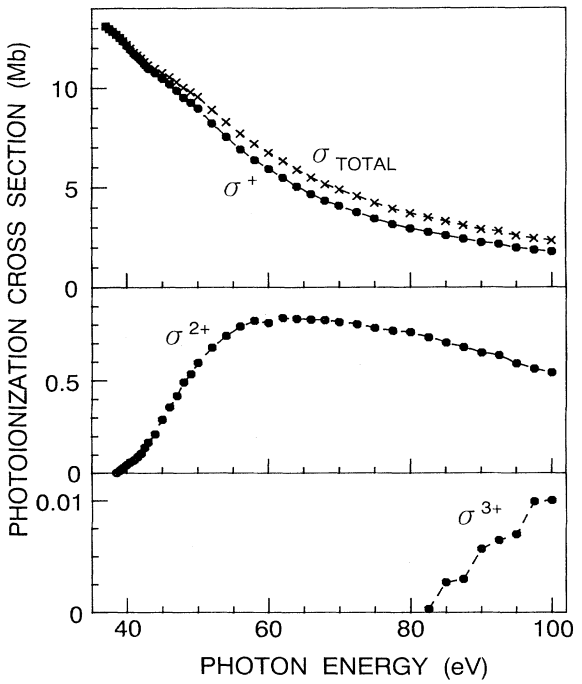

FIG. 5. Cross sections for single (σ^+), double (σ^{2+}), and triple (σ^{3+}) photoionization of CO. The total cross section (σ_{total}) is from Refs. [38,39].

should not be excluded as a possible candidate for the indirect double photoionization. In this context, it is interesting to note that three processes are in competition in the double photoionization of CO: (a) direct double photoionization, (b) indirect double photoionization (autoionization) followed by dissociation, and (c) direct dissociation of the singly charged molecular ion with subsequent autoionization in the excited atom [4].

The ratio σ^{2+}/σ^+ for CO obtained in the present study is compared with those for some other simple molecules [5,6,42] in Table II. The comparison shows that the results for CO are in close agreement with those for NO except for the ratios at 10 eV above the threshold, where the ratio for NO is larger by a factor of 1.9 than that for CO. A clear trend can be seen in Table II that the ratio σ^{2+}/σ^+ increases with the size of the molecule. The ratios summarized in Table II are considerably higher, an order of magnitude or more, than the reported values for SO_2, CO_2, and CH_4 [43–45]. However, the possibility of underestimating the ratio σ^{2+}/σ^+ for these molecules exists [6].

The threshold for the dissociative triple photoionization was observed at 82±2 eV, which is in close agreement with the 81±2 eV reported by Lablanquie *et al.* [2]. The cross section for triple photoionization is also in good agreement with that reported by Lablanquie *et al.* [2].

C. Ion branching ratios and the partial cross sections for the fragmentation of CO^+

The ion branching ratios for the precursor CO^+ obtained by the method mentioned above, determined separately from those for CO^{2+}, are shown in Fig. 6 (Table III). Three characteristic features can be seen in Fig. 6: (a) the production of the molecular CO^+ ion is the dominant process and its branching ratio exceeded 72% throughout the energy region examined, (b) a shallow minimum is found around 50 eV in the ion branching ratio of CO^+, and (c) the ion branching ratios for C^+ and O^+ are very similar in their magnitude except below 47 eV. The last feature is in sharp contrast to NO, for which a selective dissociation of NO^+ into N^+ was observed above 50 eV [5].

With respect to the dominant production of molecular CO^+, four routes should be considered: (a) configuration-interaction satellite structure ($^2\Sigma^+ 3\sigma^{-1}$, 35–45 eV) observed by photoelectron spectroscopy [46–49] and investigated theoretically [50,51] would be dissociative, (b) direct single ionization with another electron excited to high-lying electronic states (CO^{*+}) which are bound type and stable against dissociation in a μsec time scale, (c) indirect single ionization via resonant excitation to double Rydberg states (CO^{**}) of the neutral molecule, which autoionize to the high-lying bound electronic states mentioned above, and (d) double Rydberg states autoionizing to the low-lying bound electronic states, such as $X\,^2\Sigma^+$, $A\,^2\Pi$, and $B\,^2\Sigma^+$ (Ref. [7]) of CO^+. This last route implies a two-electron transition in which one electron is ionized and the other fills out a positive hole in a valence orbital. The CO^{2+} states lying between 49 and 60 eV are all dissociative [2] because of

TABLE II. Ratios of double to single photoionization above the double-photoionization threshold.

Molecule	Double-ionization threshold (eV)	10 eV	20 eV	30 eV	50 eV
CO[a]	38.4	0.054	0.131	0.193	0.285
NO[b]	38.5	0.105	0.143	0.188	0.281
OCS[c]	31.0	0.144	0.309	0.339	0.358
CS_2[d]	27.3	0.16	0.64	0.69	

[a]Present results.
[b]Reference [5].
[c]Reference [6].
[d]Reference [42].

Coulomb repulsion, and this trend may continue up to 100 eV. Higher members of the Rydberg states converging to these CO^{2+} states would also be dissociative because of a similarity of the ion core of the Rydberg states with CO^{2+}. If this is the case, routes (b) and (c) are not effective and route (d) plays an important role in the production of molecular CO^+ at higher excitation energies.

The formation of a minimum in the ion branching ratio of CO^+ around 50 eV can be interpreted in the following ways. The $^2\Sigma^+(3\sigma^{-1})$ state of CO^+ (satellite structure) would be dissociative and Rydberg states converging to repulsive CO^{2+} states would also dissociate. Because of the relative contributions of these dissociative states, the ion branching ratio for CO^+ decreases first at low-energy side. Then, new mechanisms mentioned above [(b)–(d)] open at higher energies and effectively produce the stable CO^+ ion.

The partial cross sections for the respective channels of CO^+ are shown in Fig. 7 (see Table III). Below 47 eV, the dissociation of CO^+ to C^+ is slightly preferable than O^+.

D. Ion branching ratios and the partial cross sections for the fragmentation of CO^{2+}

The ion branching ratios for the precursor CO^{2+} separately determined from those for CO^+ are shown in Fig. 8 (Table IV). The abundance of the metastable CO^{2+} increases to 10% at 45 eV in contrast to the value of 0.26% in Fig. 3, thus indicating the necessity of determining the

TABLE III. Ion branching ratios and the partial cross sections for the fragmentation of CO^+.

Photon energy (eV)	Branching ratio			Cross section (Mb)		
	C^+	O^+	CO^+	C^+	O^+	CO^+
37.0	0.091	0.060	0.850	1.20	0.78	11.12
37.5	0.097	0.065	0.838	1.26	0.84	10.86
38.0	0.102	0.071	0.827	1.30	0.91	10.60
38.5	0.107	0.075	0.818	1.36	0.95	10.35
39.0	0.111	0.077	0.812	1.39	0.96	10.14
39.5	0.114	0.082	0.804	1.40	1.01	9.91
40.0	0.116	0.086	0.798	1.40	1.05	9.66
40.5	0.119	0.089	0.791	1.42	1.06	9.43
41.0	0.121	0.091	0.788	1.42	1.06	9.22
41.5	0.121	0.096	0.783	1.40	1.11	9.04
42.0	0.124	0.099	0.776	1.42	1.13	8.83
42.5	0.125	0.102	0.773	1.40	1.14	8.63
43.0	0.126	0.105	0.770	1.38	1.15	8.45
44.0	0.130	0.113	0.757	1.40	1.21	8.13
45.0	0.130	0.116	0.753	1.36	1.22	7.88
46.0	0.134	0.123	0.743	1.37	1.25	7.56
47.0	0.137	0.129	0.734	1.35	1.27	7.24
48.0	0.139	0.132	0.730	1.32	1.25	6.95
49.0	0.140	0.134	0.726	1.30	1.24	6.72
50.0	0.139	0.134	0.726	1.25	1.21	6.51
52.0	0.135	0.131	0.734	1.11	1.08	6.03
54.0	0.135	0.126	0.739	1.01	0.95	5.57
56.0	0.128	0.120	0.752	0.88	0.83	5.19
58.0	0.124	0.115	0.762	0.78	0.73	4.84
60.0	0.124	0.113	0.763	0.73	0.67	4.52
62.0	0.119	0.110	0.772	0.65	0.60	4.22
64.0	0.115	0.105	0.780	0.58	0.53	3.93
66.0	0.109	0.099	0.792	0.51	0.46	3.68
68.0	0.107	0.094	0.799	0.46	0.41	3.45
70.0	0.106	0.092	0.802	0.43	0.37	3.26
72.5	0.101	0.086	0.813	0.38	0.32	3.05
75.0	0.099	0.082	0.820	0.34	0.28	2.80
77.5	0.096	0.081	0.823	0.30	0.26	2.59
80.0	0.094	0.078	0.829	0.27	0.23	2.43
82.5	0.094	0.077	0.829	0.26	0.21	2.28
85.0	0.096	0.077	0.827	0.25	0.20	2.13
87.5	0.095	0.079	0.826	0.23	0.19	1.99
90.0	0.095	0.080	0.826	0.21	0.18	1.84
92.5	0.097	0.082	0.821	0.21	0.18	1.76
95.0	0.099	0.080	0.821	0.20	0.16	1.62
97.5	0.096	0.086	0.818	0.18	0.16	1.52
100.0	0.098	0.089	0.812	0.17	0.16	1.44

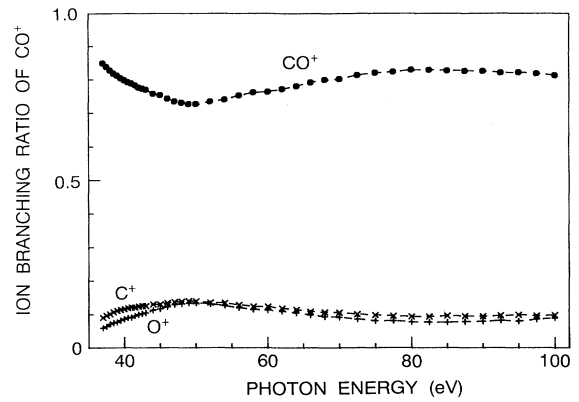

FIG. 6. Ion branching ratios of single photoionization of CO.

ion branching ratios for single and double photoionization separately. The $C^+ + O^+$ ion-pair formation is dominant because of Coulomb repulsion between two positive holes. The partial cross sections for the respective channels are shown in Fig. 9 and listed in Table V. The molecular (CO^{2+}) and dissociative ($C^+ + O^+$) double-photoionization cross sections can be compared with those reported by Lablanquie *et al.* [2].

Only the $C^+ + O^+$ ion pair is produced in double photoionization in the 38.4–41.3-eV region. The appearance potential of the molecular CO^{2+} (41.3±0.2 eV) was found to be in excellent agreement with the values of 41.25±0.05 eV recently reported by Dujardin *et al.* [24] and 40.75±0.5 eV reported by Lablanquie *et al.* [2]; both of them used synchrotron radiation, and were in slight disagreement with the value (41.8±0.3 eV) measured recently by double-charge-transfer spectroscopy [23]. Previously reported values for the threshold of the molecular CO^{2+} formation can be found in Ref. [23]. Just above the threshold of CO^{2+}, the ion branching ratio for CO^{2+} increases sharply. The predissociation of the $^1\Sigma^+_{(I)}$ (41.1 eV) and $^1\Pi_{(I)}$ (41.2 eV) states of CO^{2+} via the repulsive $^3\Sigma^-_{(I)}$ (44.4 eV) or $^3\Pi_{(I)}$ (40.6 eV) is spin forbidden and is expected to be slow [2,29]. The numerals in parentheses represent the calculated positions in the Franck-Condon region [2]. The $^1\Sigma^+_{(II)}$ (45.3 eV) state is bound [2] in the Franck-Condon region and its predissociation via $^3\Pi_{(I)}$ is also spin forbidden and parity forbidden via $^3\Sigma^-_{(I)}$. Because these CO^{2+} states produce the molecular CO^{2+}, a peak is formed in the ion branching ratio for CO^{2+} around 45 eV.

Above 50 eV, the ion branching ratio for the molecular CO^{2+} ion decreases gradually. This gradual decrease,

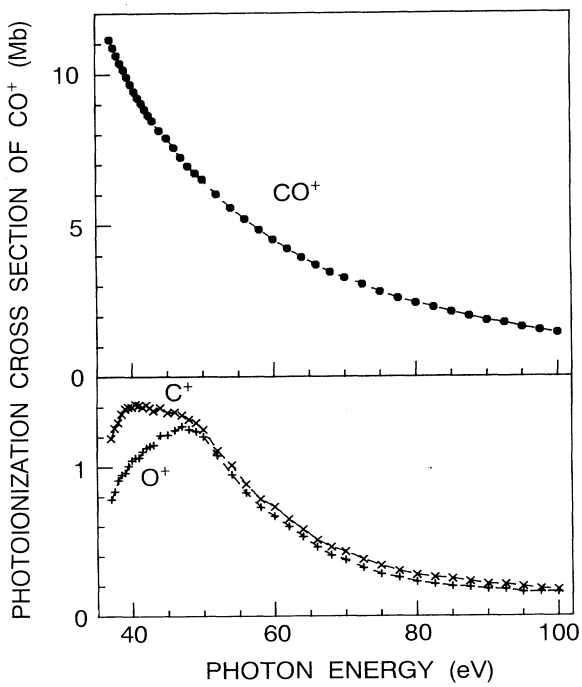

FIG. 7. Partial photoionization cross sections for the ions produced from the precursor CO^+.

TABLE IV. Ion branching ratios of CO^{2+}.

Photon energy (eV)	$C^+ + O^+$	CO^{2+}	C^{2+}	O^{2+}
38.5	1.000			
39.0	1.000			
39.5	1.000			
40.0	1.000			
40.5	1.000			
41.0	1.000			
41.5	0.975	0.025		
42.0	0.947	0.054		
42.5	0.933	0.067		
43.0	0.919	0.081		
44.0	0.895	0.106		
45.0	0.901	0.099		
46.0	0.897	0.104		
47.0	0.908	0.092		
48.0	0.919	0.081		
49.0	0.919	0.081		
50.0	0.924	0.076		
52.0	0.931	0.069		
54.0	0.936	0.064		
56.0	0.939	0.062		
58.0	0.936	0.057	0.007	
60.0	0.927	0.058	0.015	
62.0	0.922	0.054	0.024	
64.0	0.917	0.052	0.031	
66.0	0.910	0.051	0.038	
68.0	0.904	0.050	0.046	
70.0	0.898	0.049	0.053	0
72.5	0.891	0.046	0.059	0.005
75.0	0.883	0.045	0.064	0.008
77.5	0.876	0.047	0.067	0.010
80.0	0.869	0.043	0.076	0.012
82.5	0.866	0.043	0.079	0.012
85.0	0.863	0.043	0.083	0.012
87.5	0.858	0.044	0.084	0.014
90.0	0.853	0.041	0.093	0.014
92.5	0.848	0.039	0.097	0.015
95.0	0.844	0.040	0.099	0.017
97.5	0.841	0.036	0.106	0.017
100.0	0.839	0.039	0.107	0.015

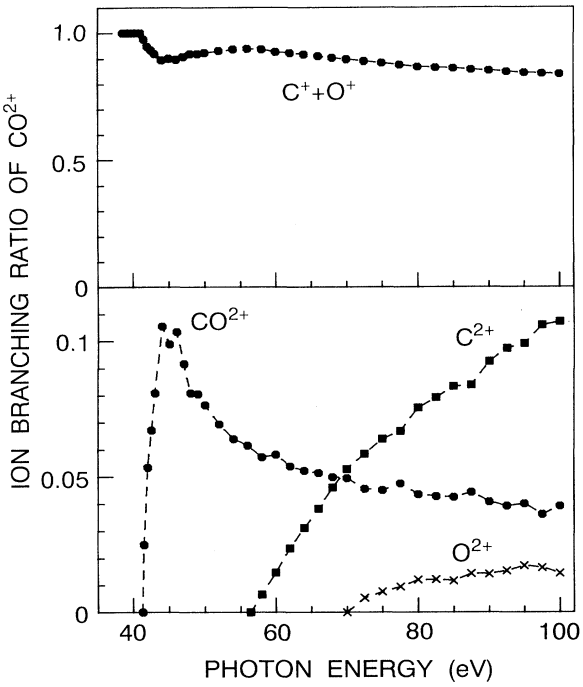

FIG. 8. Ion branching ratios of double photoionization of CO.

when compared with those for NO [5] and OCS [6], is much slower than the rapid decrease observed for NO and OCS. This gradual decrease suggests that bound or partially bound electronic states of CO^{2+} exist at the higher-energy region. Another possibility for the production of stable CO^{2+} is that the superexcited CO^{**} and

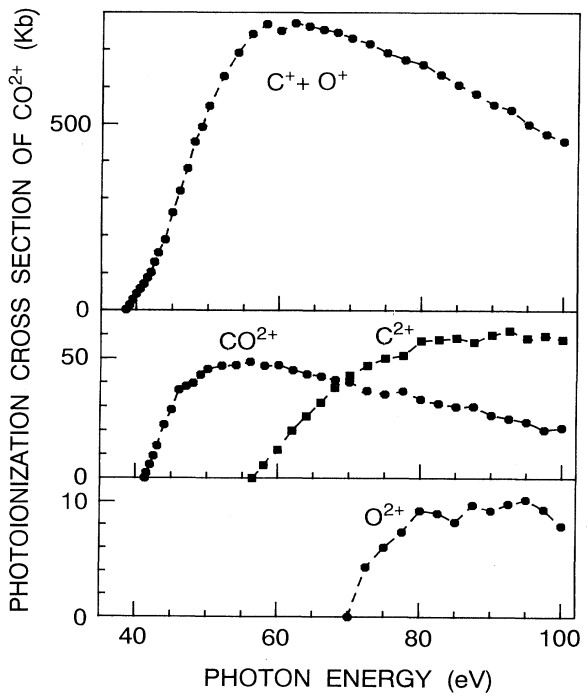

FIG. 9. Partial photoionization cross sections for the ions produced from the precursor CO^{2+}.

CO^{+*} to Rydberg states converging to high-lying electronic states of CO^{2+} autoionize by interaction with the underlying ionization continua of the low-lying quasibound state of CO^{2+} such as $^1\Sigma^+_{(I)}$, $^1\Pi_{(I)}$, and $^1\Sigma^+_{(II)}$.

The charge-localized dissociation of CO^{2+}, forming C^{2+} and O^{2+}, becomes appreciable at higher excitation energies. The appearance potentials of C^{2+} and O^{2+} are found to be 56.4±1 and 70.0±1 eV, respectively. Corresponding values of 54.2±0.2 and 61.3±0.3 eV obtained by electron impact have been reported by Hierl and Franklin [52].

E. Dissociation ratios of CO^+ and CO^{2+}

The separate determination of the ion branching ratios for the precursors CO^+ and CO^{2+} was used to obtain the dissociation ratios (ξ_s and $\xi_d+\xi_d$) of the singly and dou-

TABLE V. Partial cross sections for the fragmentation of CO^{2+} (kb).

Photon energy (eV)	$C^+ + O^+$	CO^{2+}	C^{2+}	O^{2+}
38.5	1.3			
39.0	14.5			
39.5	29.6			
40.0	45.3			
40.5	58.8			
41.0	71.7			
41.5	87.8	2.3		
42.0	103	5.8		
42.5	129	9.3		
43.0	154	13.6		
44.0	189	22.3		
45.0	261	28.6		
46.0	320	36.9		
47.0	380	38.4		
48.0	452	39.8		
49.0	493	43.2		
50.0	550	45.5		
52.0	629	46.9		
54.0	692	47.2		
56.0	742	48.6		
58.0	769	47.0	5.5	
60.0	751	47.1	12.0	
62.0	771	45.0	19.8	
64.0	763	43.4	25.9	
66.0	754	42.5	31.6	
68.0	746	41.1	38.0	
70.0	730	40.2	43.4	0
72.5	716	36.6	47.0	4.3
75.0	691	35.2	50.0	6.0
77.5	673	36.4	51.3	7.3
80.0	661	33.0	57.4	9.2
82.5	634	31.3	58.0	9.0
85.0	606	29.9	58.6	8.2
87.5	582	30.0	57.0	9.7
90.0	552	26.4	60.0	9.2
92.5	539	24.9	61.8	9.8
95.0	499	23.6	58.6	10.2
97.5	474	20.3	59.7	9.3
100.0	454	21.2	58.0	7.9

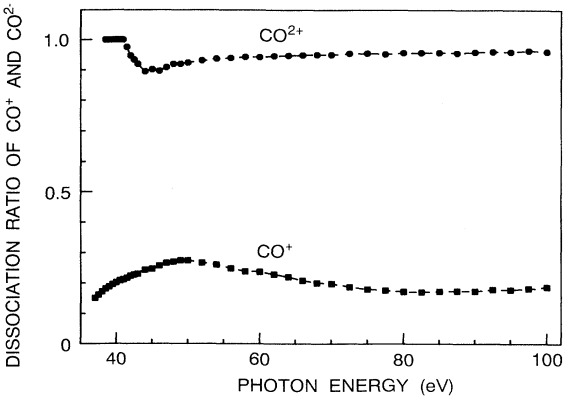

FIG. 10. Dissociation ratios of the precursors of CO^+ and CO^{2+}.

bly charged precursors, and the results are shown in Fig. 10. The dissociation ratio of CO^{2+} is larger than 0.90 throughout the region and reaches a value of about 0.95 above 55 eV. That is, atomization of CO^{2+} is the dominant process. This trend is very similar to the results obtained for OCS^{2+} [6] and NO^{2+} [5]. Although the dissociation ratio of molecular dications has been examined for only three molecules, such as OCS, NO, and CO, so far, the high dissociation ratio of dications can be regarded as a general phenomenon even if some amount of metastable dications is produced. This is because only a few low-lying electronic states of molecular dications are quasibound, if any. Conversely, the dissociation ratio of molecular cations (AB^+) splits into two groups: a high dissociation ratio in the case of OCS [6], and a low dissociation ratio (say less than 40%) for NO [5] and CO below 100 eV, although details of differentiating these two groups cannot be clearly determined at present.

V. CONCLUSIONS

By developing a method to analyze mass and PIPICO spectra, the cross sections for the single, double, and triple photoionization have been successfully determined for CO, in which both molecular and dissociative processes take place concomitantly. The method employed in the present study also makes it possible to determine the ion branching ratios and the partial cross sections for the ions produced from the precursor CO^+ separately from those of CO^{2+}, even at excitation energies where the molecular and dissociative single- and double-photoionization processes compete. It was found that in the single photoionization the production of the stable CO^+ ions is a dominant process throughout the energy region examined, whereas in the double photoionization the dissociation becomes a dominant process because of a strong Coulomb repulsion between two positive holes. For the production of the stable CO^+ and CO^{2+} ions at higher photon energies it is pointed out that the bound-type electronic states of CO^+ and CO^{2+} do exist and/or the Rydberg states play an important role through autoionization. The charge-localized dissociation of CO^{2+} leading to the production of C^{2+} and O^{2+} is also observed as a minor process in the region of the inner-valence double photoionization.

ACKNOWLEDGMENTS

Sincere gratitude is extended to the UVSOR personnel for their beneficial assistance during the experiments. This work was supported by the UVSOR Joint Research Program of the Institute for Molecular Science and in part by Grants-in-Aid for Scientific Research Grant No. 04640455 from Japan's Ministry of Education, Science and Culture.

[1] L. G. M. Pettersson, L. Karlsson, M. P. Keane, A. Naves de Brito, N. Correia, M. Larsson, L. Broström, S. Mannervik, and S. Svensson, J. Chem. Phys. **96**, 4884 (1992), and references therein.
[2] P. Lablanquie, J. Delwiche, M. J. Hubin-Franskin, I. Nenner, P. Morin, K. Ito, J. H. D. Eland, J. M. Robbe, G. Gandara, J. Fournier, and P. G. Fournier, Phys. Rev. A **40**, 5673 (1989).
[3] T. Masuoka and J. A. R. Samson, J. Chem. Phys. **74**, 1093 (1981).
[4] U. Becker, O. Hemmers, B. Langer, A. Menzel, R. Wehlitz, and W. B. Peatman, Phys. Rev. A **45**, 1295 (1992).
[5] T. Masuoka, Phys. Rev. A **48**, 1955 (1993).
[6] T. Masuoka and H. Doi, Phys. Rev. A **47**, 278 (1993).
[7] G. R. Wight, M. J. Van der Wiel, and C. E. Brion, J. Phys. B **9**, 675 (1976).
[8] F. H. Dorman and J. D. Morrison, J. Chem. Phys. **35**, 575 (1961).
[9] E. Hille and T. D. Märk, J. Chem. Phys. **69**, 4600 (1978).
[10] A. S. Newton and A. F. Sciamanna, J. Chem. Phys. **53**, 132 (1970).
[11] T. Masuoka, J. Chem. Phys. **82**, 3921 (1985).
[12] D. Mathur and J. H. D. Eland, Int. J. Mass Spectrom. Ion Processes **114**, 123 (1992).
[13] K. Siegbahn, C. Nordling, G. Johansson, J. Hedman, P. F. Heden, K. Hamrin, U. Gelius, T. Bergmark, L. O. Werme, R. Manne, and Y. Bare, *ESCA Applied to Free Molecules* (North-Holland, Amsterdam 1971).
[14] W. E. Moddeman, T. A. Carlson, M. O. Krause, B. P. Pullen, W. E. Bull, and G. K. Schweitzer, J. Chem. Phys. **55**, 2317 (1971).
[15] N. Correia, A. Flores-Riveros, H. Ågren, K. Helenelund, L. Asplund, and U. Gelius, J. Chem. Phys. **83**, 2035 (1985).
[16] J. O. K. Pedersen and P. Hvelplund, J. Phys. B **20**, L317 (1987).
[17] Z. Herman, P. Jonathan, A. G. Brenton, and J. H. Beynon, Chem. Phys. Lett. **141**, 433 (1987).
[18] M. Hamdan and A. G. Brenton, J. Phys. B **22**, L45 (1989).
[19] V. Krishnamurthi, K. Nagesha, V. R. Marathe, and D. Mathur, Phys. Rev. A **44**, 5460 (1991).
[20] S. Mazumdar, F. A. Rajgara, V. R. Marathe, C. Badrinathan, and D. Mathur, J. Phys. B **21**, 2815 (1988).
[21] P. G. Fournier, J. Phys. B **22**, L381 (1989).
[22] D. Mathur, V. R. Marathe, and S. Mazumdar, J. Phys. B

22, L385 (1989).
[23] M. L. Langford and F. M. Harris, Int. J. Mass. Spectrom. Ion Processes **124**, 241 (1993).
[24] G. Dujardin, L. Hellner, M. Hamdan, A. G. Brenton, B. J. Olsson, and M. J. Besnard-Ramage, J. Phys. B **23**, 1165 (1990).
[25] B. Brehm and G. de Frênes, Int. J. Mass Spectrom. Ion Phys. **26**, 251 (1978).
[26] J. H. Beynon, R. M. Caprioli, and J. W. Richardson, J. Am. Chem. Soc. **93**, 1852 (1971).
[27] J. M. Curtis and R. K. Boyd, J. Chem. Phys. **80**, 1150 (1984).
[28] A. C. Hurley, J. Chem. Phys. **54**, 3656 (1971).
[29] R. W. Wetmore, R. J. Le Roy, and R. K. Boyd, J. Phys. Chem. **88**, 6318 (1984).
[30] M. Larsson, B. J. Olsson, and P. Sigray, Chem. Phys. **139**, 457 (1989).
[31] V. R. Marathe and D. Mathur, Chem. Phys. Lett. **163**, 189 (1989).
[32] L. S. Cederbaum, P. Campos, F. Tarantelli, and A. Sgamellotti, J. Chem. Phys. **95**, 6634 (1991).
[33] T. Masuoka and I. Koyano, J. Chem. Phys. **95**, 909 (1991).
[34] T. Masuoka, T. Horigome, and I. Koyano, Rev. Sci. Instrum. **60**, 2179 (1989).
[35] T. Masuoka, I. Koyano, and N. Saito, Phys. Rev. A **44**, 4309 (1991).
[36] D. M. P. Holland, K. Codling, J. B. West, and G. V. Marr, J. Phys. B **12**, 2465 (1979).
[37] A. P. Hitchcock, P. Lablanquie, P. Morin, E. Lizon, A. Lugrin, M. Simon, P. Thiry, and I. Nenner, Phys. Rev. A **37**, 2448 (1988).
[38] J. A. R. Samson and J. L. Gardener, J. Electron. Spectrosc. Relat. Phenom. **8**, 35 (1976).
[39] J. A. R. Samson and G. N. Haddad (unpublished).
[40] W. F. Chan, G. Cooper, and C. E. Brion, Chem. Phys. **170**, 123 (1993).
[41] Y. Iida, F. Carnovale, S. Daviel, and C. E. Brion, Chem. Phys. **105**, 211 (1986).
[42] P. Lablanquie, I. Nenner, P. Millie, P. Morin, J. H. D. Eland, M. J. Hubin-Franskin, and J. Delwiche, J. Chem. Phys. **82**, 2951 (1985).
[43] G. Dujardin, S. Leach, O. Dutuit, P. M. Guyon, and M. Richard-Viard, Chem. Phys. **88**, 339 (1984).
[44] G. Dujardin, D. Winkoun, and S. Leach, Phys. Rev. A **31**, 3027 (1985).
[45] G. Dujardin and D. Winkoun, J. Chem. Phys. **83**, 6222 (1985).
[46] A. W. Potts and T. A. Williams, J. Electron Spectrosc. Relat. Phenom. **3**, 3 (1974).
[47] J. L. Gardner and J. A. R. Samson, J. Electron Spectrosc. Relat. Phenom. **2**, 259 (1973).
[48] S. Krummacher, V. Schmidt, F. Wuilleumier, J. M. Bizau, and D. Ederer, J. Phys. B **16**, 1733 (1983).
[49] Z. F. Liu, G. M. Bancroft, L. L. Coatsworth, and K. H. Tan, Chem. Phys. Lett. **203**, 337 (1993).
[50] J. Schirmer, L. S. Cederbaum, W. Domcke, and W. Von Niessen, Chem. Phys. **26**, 149 (1977).
[51] P. W. Langhoff, S. R. Langhoff, T. N. Rescigno, J. Schirmer, L. S. Cederbaum, W. Domcke, and W. Von Niessen, Chem. Phys. **58**, 71 (1981).
[52] P. M. Hierl and J. L. Franklin, J. Chem. Phys. **47**, 3154 (1967).